Structure of hybrid protoneutron stars within the Nambu–Jona-Lasinio model

G. F. Burgio and S. Plumari
INFN Sezione di Catania and Dipartimento di Fisica e Astronomia,
Università di Catania,
Via Santa Sofia 64, 95123 Catania, Italy
(Dated: January 20, 2014)

We investigate the structure of protoneutron stars (PNS) formed by hadronic and quark matter in β-equilibrium described by appropriate equations of state (EOS). For the hadronic matter, we use a finite temperature EOS based on the Brueckner-Bethe-Goldstone many-body theory, with realistic two- and three-body forces. For the quark sector, we employ the Nambu–Jona-Lasinio model. We find that the allowed maximum masses are comprised in a narrow range around 1.8 solar masses, with a slight dependence on the temperature. Metastable hybrid protoneutron stars are not found.

PACS numbers: 26.60.+c, 21.65.+f, 25.75.Nq, 12.39.-x

I. INTRODUCTION

Protoneutron stars are generally believed to be the evolutionary endpoints of the gravitational collapse of a massive star with mass larger than 8 solar masses [1, 2]. Several different stages may happen during the evolution process [3, 4]. Initially, a PNS is very hot, with an entropy per baryon of the order of 1 to 2, and contains neutrinos produced by electron capture in the beta-equilibrated matter. Due to their short mean free paths, they are prevented from leaving the star, and are temporarily trapped in it. The number of leptons per baryons that remain trapped is approximately 0.4. The subsequent evolution of the PNS, on a timescale of 10-20 s, is dominated by neutrino diffusion and cooling, and the newly formed neutron star (NS) stabilizes at practically zero temperature.

In a previous article [5] we have studied static properties of PNS assuming that nucleons, hyperons, and leptons are present in stellar matter. Our calculations are based on the EOS derived within the Brueckner-Bethe-Goldstone (BBG) theory of nuclear matter [6], extended to finite temperature. It turned out that for the heaviest PNS, close to the maximum mass (about two solar masses), the central particle density reaches values larger than $1/\mathrm{fm}^3$, thus making possible a hadron-quark phase transition. This could have strong consequences for the dynamical evolution of a PNS into a NS [7].

Therefore, we have extended the previous calculations, and studied hybrid protoneutron stars with a quark core described with the MIT bag model, finding maximum masses below 1.6 solar masses, independently on the temperature. Moreover, no metastable hybrid PNS were found [8].

In this paper, we discuss the structure of hybrid PNS using the BBG EOS for describing the hadronic phase, and the Nambu–Jona-Lasinio model at finite temperature for the quark matter (QM) phase. We find that no phase transition to quark matter can take place if hyperons are included in the hadronic phase, with and without neutrino trapping. Thus, the hadronic phase contains only nucleons, and as a consequence, neutrino trapping will soften the equation of state, and the PNS masses will be smaller than the NS ones.

We also find that the presence of QM limits the value of the maximum mass in a narrow interval around 1.8 $M_\odot$, with a slight dependence on the temperature.

This paper is organized as follows. In section II we review the baryonic EOS in the finite-temperature Brueckner-Hartree-Fock approach. Section III concerns the QM EOS according to the Nambu–Jona-Lasinio model, whereas section IV contains results about the hadron-quark phase transition. In section V we present the results regarding PNS structure, obtained combining the baryonic and QM EOS for beta-stable nuclear matter. Finally, in Section VI we draw our conclusions.

II. HADRONIC MATTER EQUATION OF STATE

A. The BBG theory at finite temperature

We start with the description of the hadronic phase. The EOS is based on the non-relativistic Brueckner-Bethe-Goldstone (BBG) many-body theory [6], which is a linked cluster expansion of the energy per nucleon of nuclear matter, well convergent [9] and accurate enough in the density range relevant for neutron stars.

At finite temperature, the formalism which is closest to the BBG expansion, and actually reduces to it in the zero-temperature limit, is the one formulated by Bloch and De Dominicis in [10]. This has been applied successfully to the study of the limiting temperature in nuclei [11].In this approach the essential ingredient is the two-body scattering matrix K, which, along with the single-particle potential U, satisfies the self-consistent equations

$$\begin{aligned}\langle k_1k_2|K(W)|k_3k_4\rangle &= \langle k_1k_2|V|k_3k_4\rangle \\ &+ \mathrm{Re}\sum_{k_3'k_4'}\langle k_1k_2|V|k_3'k_4'\rangle\frac{[1-n(k_3')][1-n(k_4')]}{W-E_{k_3'}-E_{k_4'}+i\varepsilon}\langle k_3'k_4'|K(W)|k_3k_4\rangle\end{aligned} \tag{1}$$

and

$$U(k_1)=\sum_{k_2}n(k_2)\langle k_1k_2|K(W)|k_1k_2\rangle_A\,, \tag{2}$$

where k_i generally denote momentum, spin, and isospin. $W=E_{k_1}+E_{k_2}$ represents the starting energy, $E_k=k^2/2m+U(k)$

the single-particle energy, and $n(k)$ is a Fermi distribution. For the two-body interaction V, we choose the Argonne V_{18} nucleon-nucleon potential [12]. We have also introduced three-body forces (TBF) among nucleons, adopting the phenomenological Urbana model [13]. This allows to reproduce correctly the nuclear matter saturation point $\rho_0 \approx 0.17$ fm^{-3}, $E/A \approx -16$ MeV, and gives values of incompressibility and symmetry energy at saturation compatible with those extracted from phenomenology [14]. For details, the reader is referred to Ref.[15].

The calculation of stable configurations in PNS requires the knowledge of the EOS at different chemical compositions. In order to simplify the numerical procedure, we have introduced the so-called *Frozen Correlations Approximation*, i.e., the correlations at $T \neq 0$ are assumed to be essentially the same as at $T = 0$. This means that the single-particle potential $U_i(k)$ for the component i can be approximated by the one calculated at $T = 0$. It has been shown in ref. [6] that this assumption is valid with good accuracy if the temperature is not too high. Within this approximation, for given density and temperature, Eqs. (1) and (2) have to be solved self-consistently along with the equations for the densities, $\rho_i = \sum_k n_i(k)$, and the free energy density, which has the following simplified expression

$$f = \sum_i \left[\sum_k n_i(k) \left(\frac{k^2}{2m_i} + \frac{1}{2} U_i(k) \right) - T s_i \right] , \qquad (3)$$

where

$$s_i = -\sum_k \Big(n_i(k) \ln n_i(k) + [1 - n_i(k)] \ln[1 - n_i(k)] \Big) \qquad (4)$$

is the entropy density for component i treated as a free gas with spectrum $E_i(k)$. In recent years, the BBG approach at zero temperature has been extended to the hyperonic sector in a fully self-consistent way [16, 17], by including the Σ^- and Λ hyperons. For that, we have used the Nijmegen soft-core nucleon-hyperon (NH) potentials NSC89 [18], and neglected the hyperon-hyperon (HH) interactions, since so far no reliable HH potentials are available. We have found that the presence of hyperons strongly softens the EOS, and produces a maximum NS mass that lies slightly below the canonical value of 1.44 $M_\odot$ [19]. However, since the quantitative effects of more reliable NH and HH potentials haven't been explored yet, in this paper we discuss finite temperature calculations by using non-interacting hyperons. This approximation could not be justified for the present work, because the hadron-quark phase transition occurs at densities much above the normal nuclear matter saturation density, where hyperons are expected to play a role. A more complete study with the inclusion of interacting hyperons at finite temperature is in progress.

For stars in which the strongly interacting particles are only baryons, the composition at given baryon density ρ is determined by imposing electric charge neutrality and equilibrium under the weak processes

$$B_1 \to B_2 + l + \overline{\nu}_l \ , \quad B_2 + l \to B_1 + \nu_l \ , \qquad (5)$$

where B_1 and B_2 are baryons and l is a lepton, either an electron or a muon. When the neutrinos are trapped, these two requirements imply that the relations

$$\sum_i q_i x_i + \sum_l q_l x_l = 0 \qquad (6)$$

and

$$\mu_i = b_i \mu_n - q_i (\mu_l - \mu_{\nu_l}) \, , \qquad (7)$$

are satisfied. In the expression above, $x_i = \rho_i/\rho$ is the baryon fraction of the species i, b_i the baryon number, and q_i the electric charge. Equivalent quantities are defined for the leptons $l = e, \mu$. The initial PNS contains trapped neutrinos produced in electron capture process, so the electron and muon lepton numbers are conserved on dynamical time scales. We fix the electron lepton number $Y_e = x_e + x_{\nu_e} = 0.4$, as indicated by gravitational collapse calculations, and $Y_\mu = x_\mu - x_{\overline{\nu}_\mu} = 0$, since no muons are present when neutrinos become trapped.

Hence, the composition of beta-stable and charge-neutral baryonic matter is determined by the baryon chemical potentials for each species i, which are related to the free energy density

$$\mu_i = \frac{\partial f}{\partial \rho_i} \, , \qquad (8)$$

Therefore, one needs to know the functional dependence of the free energy, Eq. (3), on the individual partial densities ρ_i and on the temperature. In Ref. [5] we have provided analytical parametrizations of our numerical results for symmetric and neutron matter, from which one can readily obtain the nucleon chemical potentials in beta-stable matter. The chemical potentials of the noninteracting hyperons and leptons are obtained by solving numerically the free Fermi gas model at finite temperature.

Once the composition of the β-stable, charge neutral stellar matter is known, one can calculate the total free energy density f and then the pressure p through the usual thermodynamical relation

$$p = \rho^2 \frac{\partial (f/\rho)}{\partial \rho} \, . \qquad (9)$$

The resulting EOS is displayed in Fig. 1, where the pressure for beta-stable matter, without (solid lines) and with (dashed lines) neutrinos, is plotted as a function of the baryon density at temperature T = 30 MeV. The upper curves represent the EOS for stellar matter containing nucleons only, whereas the lower curves display the case when free hyperons are included. We notice that if only nucleons and leptons are present in the neutrino-trapped matter, the EOS gets softer because nuclear matter is more symmetric. The presence of hyperons introduces additional softening. However, the degree of softening is smaller in the neutrino-trapped case than in the neutrino-free case, because the hyperons appear at larger densities in neutrino-trapped matter, and their concentration is smaller. We have checked that this trend depends weakly on the temperature, which plays a role only in the low density range.

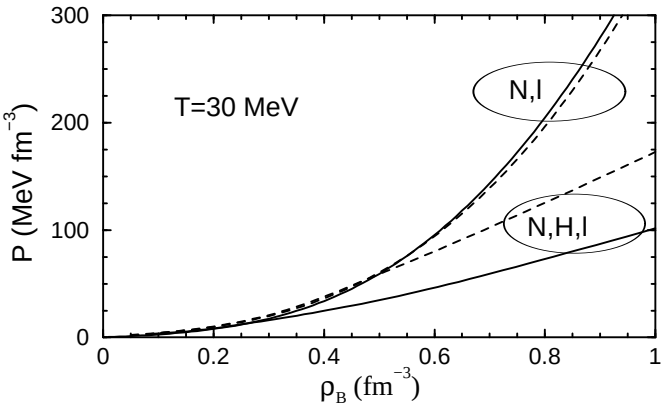

FIG. 1: The EOS in beta-stable baryon matter is displayed for temperature T = 30 MeV. The upper curves display results for matter containing nucleons and leptons, whereas the lower curves are for matter with hyperons. Solid (dashed) lines refer to the neutrino-free (neutrino-trapped) case.

III. QUARK MATTER EQUATION OF STATE

A. The Nambu–Jona-Lasinio model

We describe the quark phase within the Nambu–Jona-Lasinio model [20, 21]. The SU(3) version of the model includes most of symmetries of the QCD Lagrangian, including the spontaneous breakdown of chiral symmetry, which is essential in treating the lightest hadrons. The NJL model assumes deconfined point-like quarks, and is not renormalizable, requiring regularization through a cutoff in three momentum space. In its commonly used form, the Lagrangian reads

$$\begin{aligned}\mathscr{L} &= \bar{q}(i\gamma^\mu\partial_\mu - \hat{m})q + G\sum_{a=0}^{8}\left[(\bar{q}\tau_a q)^2 + (\bar{q}i\gamma_5\tau_a q)^2\right] \\ &- K\left\{\det{}_f[\bar{q}(1+\gamma_5)q] + \det{}_f[\bar{q}(1-\gamma_5)q]\right\}, \qquad (10)\end{aligned}$$

where q are the quark fields with three flavors and three colors, and τ_a are the U(3) flavor matrices. The model parameters are the current quark mass matrix $\hat{m} = \mathrm{diag}(m_u, m_d, m_s)$, the coupling constants G and K, and the cutoff in the three-momentum space, Λ. Following ref.[20], we choose $\Lambda = 602.3$ MeV, the two coupling constants $G = 1.835/\Lambda^2$ and $K = 12.36/\Lambda^5$, as well as the current quark masses $m_u = m_d = 5.5$ MeV, $m_s = 140.7$ MeV. The values chosen for those parameters have been adjusted to reproduce masses and decay constants of the pseudoscalar meson nonet.

In the mean-field approximation at finite temperature and chemical potential, the thermodynamical potential of the quark phase is $\Omega = \Omega_{\rm FG} + \Omega_{\rm Int}$, where

$$\frac{\Omega_{\rm FG}}{V}(T,\mu_i) = 2N_c T\sum_{i=u,d,s}\int\frac{d^3p}{(2\pi)^3}\left[\ln(1-f_i)+\ln(1-\tilde{f}_i)\right] \qquad (11)$$

is the Fermi gas contribution arising from quarks. We consider three flavors and three colors, hence $N_c = 3$. The distribution functions of fermions and anti-fermions are given by $f_i = [1+\exp(\frac{1}{T}(E_i-\mu_i))]^{-1}$ and $\tilde{f}_i = [1+\exp(\frac{1}{T}(E_i+\mu_i))]^{-1}$. E_i and μ_i denote the single particle energy and chemical potential of the quark flavor i.

The thermodynamical potential due to interactions among quarks is given by

$$\begin{aligned}\frac{\Omega_{\rm Int}}{V}(T,\mu_i) &= -2N_c\sum_{i=u,d,s}\int\frac{d^3p}{(2\pi)^3}\left(\sqrt{M_i^2+p^2}-\sqrt{m_i^2+p^2}\right) \\ &+ 2G<\bar{q}_i q_i>^2 \\ &- 4K<\bar{q}_u q_u><\bar{q}_d q_d><\bar{q}_s q_s> \qquad (12)\end{aligned}$$

In the NJL model, the quark masses are dynamically generated as solutions of the gap equation, obtained by imposing that the potential be stationary with respect to variations in the quark condensate $<\bar{q}_i q_i>$, thus finding

$$M_i = m_i - 4G<\bar{q}_i q_i>^2 + 2K<\bar{q}_j q_j><\bar{q}_k q_k> \qquad (13)$$

being $(q_i, q_j, q_k) =$ any permutation of (u,d,s). The quark condensate $<\bar{q}_i q_i>$ and the quark number density n_i are given respectively by

$$\begin{aligned}<\bar{q}_i q_i> &= -2N_c\int\frac{d^3p}{(2\pi)^3}\frac{M_i}{E_i}\left[1-f_i-\tilde{f}_i\right], \\ n_i &= 2N_c\int\frac{d^3p}{(2\pi)^3}\left[f_i-\tilde{f}_i\right]. \qquad (14)\end{aligned}$$

Eq.(14) has to be evaluated self-consistently with Eq.(13), forming a set of six coupled equations for the constituent masses M_i. Once the self-consistent solutions are found, we can calculate the pressure and the energy density through the usual thermodynamical relations

$$p = -\Omega, \qquad \varepsilon = \Omega + Ts + \sum_i \mu_i n_i \qquad (15)$$

where $s = \partial\Omega/\partial T$ is the entropy density and $n_i = -\partial\Omega/\partial\mu_i$ are the number densities of flavor i. The total quark number density and the baryon number density are given by $n = \sum_i n_i$ and $\rho_B = n/3$, respectively. The reader can find more details in ref.[21].

In a PNS with quark matter and trapped neutrinos we must impose beta equilibrium, charge neutrality, and baryon and lepton number conservation. More precisely, the individual quark chemical potentials are fixed by Eq. (7) with $b_q = 1/3$, which implies

$$\mu_d = \mu_s = \mu_u + \mu_l - \mu_{\nu_l}. \qquad (16)$$

The charge neutrality condition and the total baryon number conservation read

$$\begin{aligned}n_e + n_\mu &= \frac{1}{3}(2n_u - n_d - n_s), \qquad (17)\\ 3\rho_B &= n_u + n_d + n_s. \qquad (18)\end{aligned}$$

These equations determine the composition and the pressure of the quark matter phase.

Let us discuss first the main features of beta-equilibrated and charge neutral quark matter within the NJL model. In Fig. 2 we show particle fractions $x_i = \rho_i/\rho$ as a function of the baryon density for neutrino-free (upper and middle panels), and neutrino-trapped quark matter (lower panel). At zero temperature, we observe a substantial amount of u and d quarks, whereas the s-quark starts to appear at baryon density four times larger than the normal saturation value. With increasing density, the s-quark population keeps smaller than the u and d populations. With increasing temperature, we observe a slight change of the particle population mainly at low density, because of the tails in the Fermi distributions. In this case, the onset for s-quarks takes place at density smaller than in the cold case. The presence of neutrinos influences quite strongly the composition, as displayed in the lower panel of Fig. 2. In this case the relative fraction of u quarks increases substantially from 33% to about 42%, compensating the charge of the electrons that are present at an average percentage of 8% throughout the considered range of baryon density, whereas the d and s quark fractions decrease. This implies that in the neutrino trapped case, being the strangeness content smaller than in the neutrino-free case, the equation of state for quark matter will be stiffer. This is indeed shown in Fig. 3, where the pressure is displayed as a function of the mass-energy density for the neutrino-free (lower curves), and for neutrino-trapped case (upper curve). The behaviour of the pressure is consequence of the quark population in beta-stable matter. We clearly observe a kink in the pressure, corresponding to the onset of the s-quark. The kink becomes smoother in the neutrino-trapped case, because the s-quark concentration is smaller. Moreover, the EOS for β-stable, charge neutral quark matter derived within the NJL model shows a clear dependence on the trapped lepton fraction. This is different from the EOS derived with the MIT bag model for describing the quark phase, where no dependence on the trapped lepton fraction is actually found [8, 22].

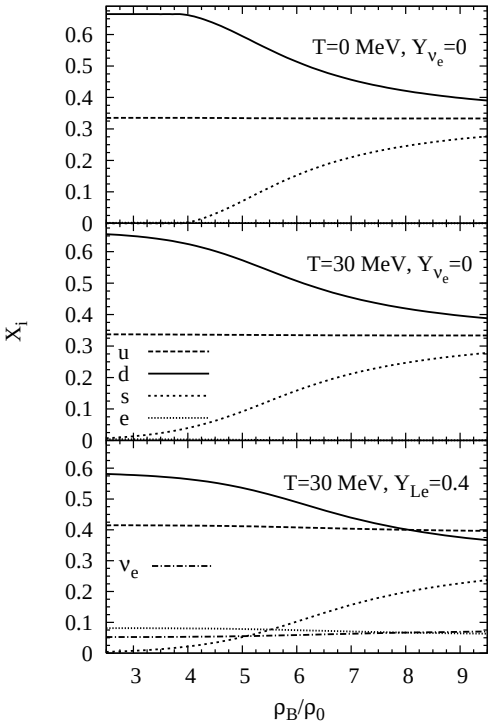

FIG. 2: The fraction of u,d,s quarks is displayed as a function of baryon density for several cases, i.e. $T = 0$ (upper panel), and $T = 30$ MeV (middle panel) without neutrino trapping. The case for $T = 30$ MeV with neutrino trapping is shown in the lower panel.

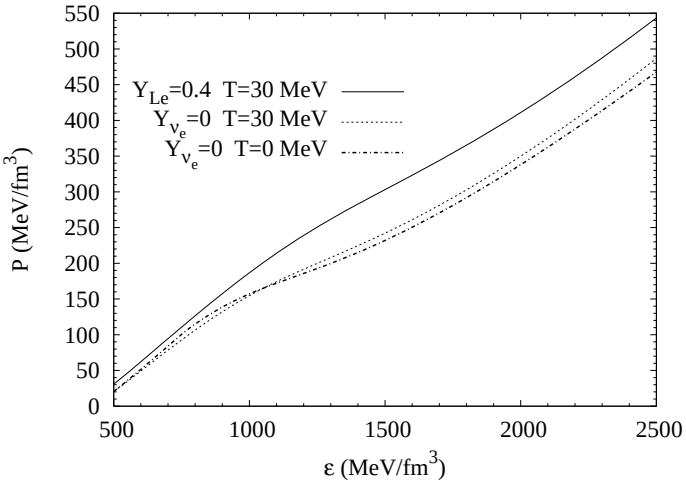

FIG. 3: Pressure as a function of the mass-energy density for beta-stable, charge neutral quark matter. See text for details.

IV. PHASE TRANSITION IN HOT BETA-STABLE MATTER

In order to perform the hadron-quark phase transition in beta-stable matter at finite temperature, we adopt the simple Maxwell construction. The more general Gibbs construction [23, 24] is still affected by many theoretical uncertainties [25], and in any case the final mass-radius relation of massive (proto)neutron stars [26] is slightly affected.

Assuming a first-order phase transition, we impose thermal, chemical, and mechanical equilibrium between the two phases. This implies that the phase coexistence is determined by a crossing point in the pressure vs. chemical potential plot, as shown in Fig. 4. There we display the pressure p as function of the baryon chemical potential μ_B for baryonic and quark matter phases at temperatures $T = 0,\ 30$ MeV. In the upper panel we show the case at $T = 0$ without neutrinos. The solid line represents the calculations performed with the BBG method with only nucleons, the dot-dashed line displays the case when free hyperons are included, and the dashed line is the NJL calculation. We observe that the phase transition, marked by a full dot, occurs if only nucleons are present in baryonic matter, as it was already found in ref.[27]. In the BHF approach, this is due to the strong softening of the baryonic equation of state when hyperons are included. The same holds true at finite temperature, without and with neutrino trapping, as clearly shown in Fig. 4. In the middle panel,

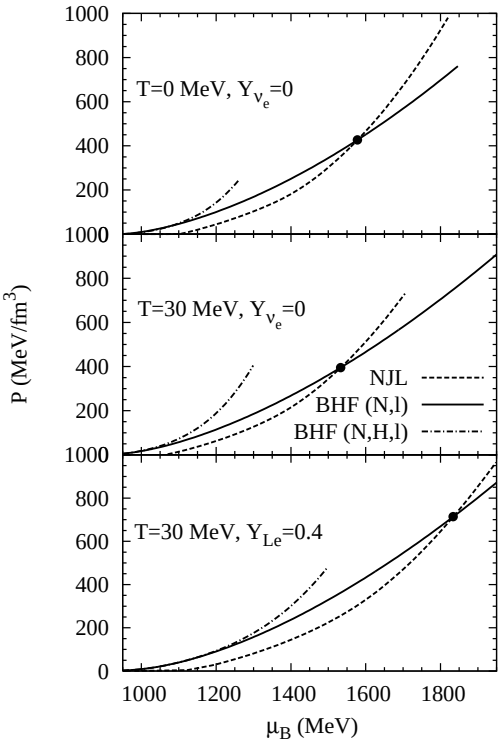

FIG. 4: Pressure as a function of the baryon chemical potential for beta-stable, charge neutral nuclear matter and quark matter. See text for details.

we display results at $T = 30$ MeV without neutrino trapping. We observe that the crossing point is only slightly affected by thermal effects, and is shifted towards smaller values of the chemical potential. This means that the phase transition starts at a baryon density smaller than in the cold case. Finally, in the lower panel, we display the neutrino-trapped case at $T = 30$ MeV. Neutrino trapping makes the baryonic EOS softer and the quark matter EOS stiffer, hence the phase transition is shifted at larger values of the chemical potential, and of the baryon density.

In Fig. 5 we display the pressure as a function of the baryon density for the several cases discussed above. The plateaus are consequence of the Maxwell construction. Below the plateau, β-stable and charge neutral stellar matter is in the purely hadronic phase, whereas for density above the ones characterizing the plateau, the system is in the pure quark phase. We notice the neutrino trapping shifts the quark matter onset at larger values, and gives rise to a wider plateau.

Similar calculations have been performed in ref.[28], where the non linear Walecka model [29] has been adopted for the hadronic phase, which includes nucleons and hyperons, and the NJL model with a different choice of the parameters for the description of the quark phase. The phase transition between the two phases has been performed adopting the Gibbs construction. Also in this case, the onset of quark matter appears at values of the baryon density which decrease with increasing the temperature. If neutrino trapping is taken into account, the onset of quark matter is shifted at larger values of

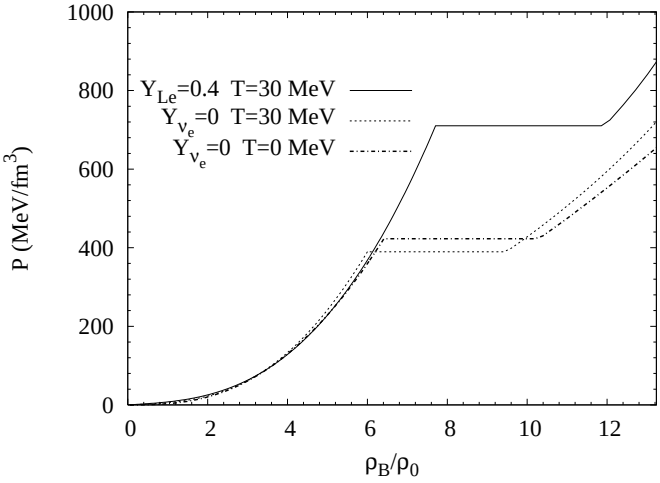

FIG. 5: Pressure as a function of the baryon density, normalized with respect to the nuclear matter saturation density ρ_0.

the baryon density. In general, the larger the temperature, the smaller is the density of quark matter onset. We notice that, in spite of the different theoretical framework, we obtain quite similar results.

V. PROTONEUTRON STAR STRUCTURE

Based on these results for the beta-stable baryon and QM phases, we can now determine the properties of static (proto)-neutron stars. The stable configurations can be obtained from the well-known Tolman-Oppenheimer-Volkoff (TOV) equations [1] for the pressure p and the enclosed mass m,

$$\frac{dp(r)}{dr} = -\frac{Gm(r)\varepsilon(r)}{r^2}\frac{\left[1+\frac{p(r)}{\varepsilon(r)}\right]\left[1+\frac{4\pi r^3 p(r)}{m(r)}\right]}{1-2Gm(r)/r}, \qquad \frac{dm(r)}{dr} = 4\pi r^2\varepsilon(r), \tag{19}$$

once the EOS $p(\varepsilon)$ is specified, being ε the total energy density (G is the the gravitational constant). Starting with a central energy density $\varepsilon(r=0) \equiv \varepsilon_c$, the numerical integration of eqs.(19) provides the mass-radius relation.

Simulations of supernovae explosions [4, 30] show that during the early stage, the entropy profile decreases from the surface to the core starting from values of 6–10 [4], and the temperature drops rapidly to zero at the surface of the star due to the fast cooling of the outer part of the PNS, where the stellar matter is transparent to neutrinos. Therefore, we have modelled the PNS by assuming a hot isothermal and neutrino-opaque core separated from an outer cold crust [31, 32] by an isentropic, beta-equilibrated, and neutrino-free intermediate layer described by the Lattimer and Swesty equation of state [33]. For details, the reader is referred to ref.[8, 34].

In the following we consider two snapshots which represent the thermodynamical conditions in an evolving PNS : i) the initial state consisting of a PNS with a hot ($T_{\rm core} \approx 30$–40 MeV) neutrino-trapped core and a high-entropy transition

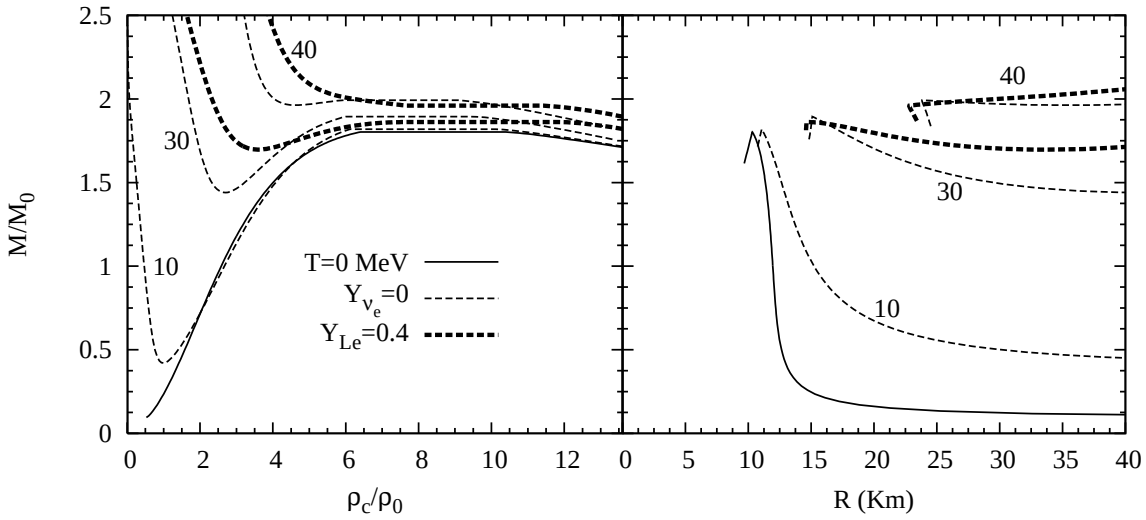

FIG. 6: The mass-central density (radius) relation is displayed in the left (right) panel. The mass is given in units of the solar mass $M_\odot = 1.989 \times 10^{33}$g, and the central density ρ_c is normalized with respect to the saturation value $\rho_0 = 0.17$ fm^{-3}.

layer ($S_{\rm env.} \approx$ 6–8), joined to a cold outer crust; ii) the final state which represents the short-term cooling, where the neutrino-free core possesses a low temperature of about 10 MeV and is direcly attached to a cold crust.

The results are plotted in Fig. 6, where we display the gravitational mass M_G (in units of the solar mass $M_\odot$) as a function of the central baryon density ρ_c (left panels) and the radius R (right panels). We display the complete set of results at core temperatures $T = 0,\ 10$ MeV without neutrino trapping, and $T = 30,\ 40$ MeV without and with neutrino trapping. Due to the Maxwell construction, the curves are not continuous and display plateaus in the mass-central density relation, which disappear in the case of the Gibbs construction. For values of central density smaller than the one characterizing the maximum mass, the PNS are purely baryonic stars. Then an increase of central density is required in order to start the quark phase, as shown by the phase diagram of Fig.5. We find that the onset of the pure quark phase at the center of the PNS as the mass increases marks an instability of the star, i.e. the PNS collapses to a black hole at the transition point since the quark EoS is unable to sustain the increasing central pressure due to gravity. We had already found the same results in the case at T=0 [27]. It has been argued that this instability might be related to the lack of confinement in the original NJL model [35]. Thus, heavy hybrid PNS in this model are practically baryonic stars up to large values of the central densities, eventually with a core in a mixed hadron-quark phase. The characteristics of the maximum mass configurations are reported separately in Table I. We notice that the maximum PNS masses are comprised in a small range around 1.8 solar masses, with a slight dependence on the temperature. Moreover, they turn out to be smaller than those of cold NS. This is due to the fact that the baryonic phase contains only nucleons, in which case neutrino trapping softens the EOS. This leads to smaller maximum masses, and excludes the possibility of metastable configurations.

Composition	T (MeV)	$M_G/M_\odot$	R (km)	ρ_c/ρ_0	ε_c(MeV/fm^3)
	0	1.8	10.3	6.4	1294
N, QM, l	10	1.82	11.	6.12	1217
	30	1.9	15.	6.	1168
	40	1.99	23.8	5.94	1138
	0	1.76	9.4	7.82	1751
N, QM, l, ν_e	10	1.78	10.9	7.76	1730
	30	1.86	14.6	7.7	1689
	40	–	–	–	–

TABLE I: Properties of the maximum mass configuration for different stellar compositions and temperatures.

Below the maximum mass configuration, however, the stars develop an extended outer envelope of hot matter, the details of which depend on the treatment of the low-density baryonic phase. The temperature dependence of the curves is quite pronounced for intermediate and low-mass stars, showing a strong increase of the minimum mass with temperature. Above core temperatures of about 40 MeV all stellar configurations become unstable.

VI. CONCLUSIONS

In this article we have studied hybrid PNS, combining the most recent microscopic baryonic EOS in the BBG approach at finite temperature with the Nambu–Jona-Lasinio model for describing the QM phase. Within this approach, we have found that the hadron-quark phase transition can take place if baryonic matter contains only nucleons. The inclusion of free hyperons softens considerably the EOS, and there-

fore inhibits any phase transition to quark matter. This is in agreement with the findings obtained at $T = 0$ in Ref.[27], where the Njimegen soft-core nucleon-hyperon interaction was included. This requires new experimental data on hypernuclei, from which more modern parametrizations of the nucleon-hyperon and/or hyperon-hyperon interaction may be extracted.

Within the NJL model for quark matter, we have also found the following : i) the transition density to the quark phase in neutrino-free baryonic matter occurs at about 6 times normal nuclear matter saturation density; ii) with increasing temperature, the onset is shifted to smaller and smaller values of the baryon density, and iii) neutrino trapping substantially increases the transition density to QM.

Therefore the hadron-quark phase transition studied with the original NJL model possesses general features, which are quite similar to the ones found with the MIT bag model [8], where an increase of the temperature shifts the transition density to lower values. Moreover, in this approach, hyperons are present in the hadron-quark mixed phase.

We have also found that maximum mass for hybrid PNS lie in a narrow range around 1.8 solar masses, and that they are smaller than the corresponding ones obtained in the cold, neutrino-free case. Therefore, metastable configurations are not possible. This same result was found in ref.[8], where the MIT bag model was employed for describing the quark phase. Both results are is in contrast to Ref. [7], where such metastability was found for hybrid stars, but with a much stiffer baryonic EOS including hyperons.

Again, we confirm our prediction of limiting masses for PNS smaller than 2 solar masses, which are compatible with currently established observational data on NS.

Acknowledgments

We warmly thank J. Pons (University of Alicante, Spain) and M. Baldo (INFN Sezione di Catania, Italy) for fruitful discussions.

[1] S. L. Shapiro and S. A. Teukolsky, *Black Holes, White Dwarfs, and Neutron Stars* (John Wiley and Sons, New York, 1983).
[2] H. A. Bethe, Rev. Mod. Phys. **62**, 801 (1990).
[3] M. Prakash, I. Bombaci, M. Prakash, P. J. Ellis, J. M. Lattimer, and R. Knorren, Phys. Rep. **280**, 1 (1997).
[4] A. Burrows and J. M. Lattimer, Astrophys. J. **307**, 178 (1986).
[5] O. E. Nicotra, M. Baldo, G. F. Burgio, and H. J. Schulze, Astron. Astrophys. **451**, 213 (2006).
[6] M. Baldo, *Nuclear Methods and the Nuclear Equation of State*, International Review of Nuclear Physics, Vol. 8 (World Scientific, Singapore, 1999).
[7] M. Prakash, J. R. Cooke, and J. M. Lattimer, Phys. Rev. **D52**, 661 (1995); A. W. Steiner, M. Prakash, and J. M. Lattimer, Phys. Lett. **B486**, 239 (2000); J. A. Pons, A. W. Steiner, M. Prakash, and J. M. Lattimer, Phys. Rev. Lett. **86**, 5223 (2001).
[8] O. E. Nicotra, M. Baldo, G. F. Burgio, and H. J. Schulze, Phys. Rev. **D74**, 123001 (2006).
[9] B. D. Day, Phys. Rev. **C24**, 1203 (1981); H. Q. Song, M. Baldo, G. Giansiracusa, and U. Lombardo, Phys. Rev. Lett. **81**, 1584 (1998); M. Baldo, G. Giansiracusa, U. Lombardo, and H. Q. Song, Phys. Lett. **B473**, 1 (2000).
[10] C. Bloch and C. De Dominicis, Nucl. Phys. **7**, 459 (1958); **10**, 181,509 (1959).
[11] M. Baldo and L. S. Ferreira, Phys. Rev. **C59**, 682 (1999); M. Baldo, L. S. Ferreira, and O. E. Nicotra, Phys. Rev. **C69**, 034321 (2004).
[12] R. B. Wiringa, V. G. J. Stoks, and R. Schiavilla, Phys. Rev. **C51**, 38 (1995).
[13] J. Carlson, V. R. Pandharipande, and R. B. Wiringa, Nucl. Phys. **A401**, 59 (1983); R. Schiavilla, V. R. Pandharipande, and R. B. Wiringa, Nucl. Phys. **A449**, 219 (1986).
[14] W. D. Myers and W. J. Swiatecki, Nucl. Phys. **A601**, 141 (1996); Phys. Rev. **C57**, 3020 (1998).
[15] M. Baldo, I. Bombaci, and G. F. Burgio, Astron. Astrophys. **328**, 274 (1997); X. R. Zhou, G. F. Burgio, U. Lombardo, H.-J. Schulze, and W. Zuo, Phys. Rev. **C69**, 018801 (2004).
[16] H.-J. Schulze, A. Lejeune, J. Cugnon, M. Baldo, and U. Lombardo, Phys. Lett. **B355**, 21 (1995); H.-J. Schulze, M. Baldo, U. Lombardo, J. Cugnon, and A. Lejeune, Phys. Rev. **C57**, 704 (1998).
[17] M. Baldo, G. F. Burgio, and H.-J. Schulze, Phys. Rev. **C58**, 3688 (1998); Phys. Rev. **C61**, 055801 (2000).
[18] P. M. M. Maessen, Th. A. Rijken, and J. J. de Swart, Phys. Rev. **C40**, 2226 (1989).
[19] R. A. Hulse and J. H. Taylor, Astrophys. J. **195**, L51 (1975); J. H. Taylor and J. M. Weisberg, Astrophys. J. **345**, 434 (1989).
[20] S. P. Klevansky, Rev. Mod. Phys. **64**, 649 (1992); P. Rehberg, S. P. Klevansky, J. Hüfner, Phys. Rev. **C53**, 410 (1996).
[21] M. Buballa, Phys. Rept. **407**, 205 (2005).
[22] D. P. Menezes, C. Providência, and D. B. Melrose, J. Phys. G **32**, 1081 (2006).
[23] N. K. Glendenning, *Compact Stars, Nuclear Physics, Particle Physics, and General Relativity*, 2nd ed. (Springer, New York, 2000).
[24] N. K. Glendenning, Phys. Rev. **D46**, 1274 (1992).
[25] T. Endo, T. Maruyama, S. Chiba, and T. Tatsumi, Prog. Theor. Phys. **115**, 337 (2006).
[26] G. F. Burgio, M. Baldo, P. K. Sahu, A. B. Santra, and H.-J. Schulze, Phys. Lett. **B526**, 19 (2002); G. F. Burgio, M. Baldo, P. K. Sahu, and H.-J. Schulze, Phys. Rev. **C66**, 025802 (2002).
[27] M. Baldo, M. Buballa, G. F. Burgio, F. Neumann, M. Oertel, and H.-J. Schulze, Phys. Lett. **B562**, 153 (2003).
[28] D. P. Menezes and C. Providência, Phys. Rev. **C68**, 035804 (2003); Phys. Rev. **C69**, 045801 (2004).
[29] B. D. Serot and J. D. Walecka, Adv. Nucl. Phys. **16**, 1 (1986).
[30] J. A. Pons, S. Reddy, M. Prakash, J. M. Lattimer, and J. A. Miralles, Astrophys. J. **513**, 780 (1999); L. Villain, J. A. Pons, P. Cerdá-Durán, and E. Gourgoulhon, Astron. Astrophys. **418**, 283 (2004).
[31] G. Baym, C. Pethick, and D. Sutherland, Astrophys. J. **170**, 299 (1971).
[32] R. Feynman, F. Metropolis, and E. Teller, Phys. Rev. **C75**, 1561 (1949).
[33] J. M. Lattimer and F. D. Swesty, Nucl. Phys. **A535**, 331 (1997).

[34] O. E. Nicotra, arXiv:nucl-th/0607055.
[35] M. Baldo, G.F. Burgio, P. Castorina, S. Plumari, and D. Zappala', Phys. Rev. **C75**, 035804 (2007), and references therein.